# Magnetic resonance elastography: evaluation of new inversion algorithm and quantitative analysis method

Annelise M. Silva,[5] Roger C. Grimm,[1] Kevin J. Glaser,[1] Yinlin Fu,[4] Teresa Wu,[4]
Richard L. Ehman,[1,2] Alvin C. Silva[3]

[1]Department of Radiology, Mayo Clinic, Rochester, MN, USA
[2]Department of Physiology and Biomedical Engineering, Mayo Clinic, Rochester, MN, USA
[3]Department of Radiology, Mayo Clinic, 13400 E Shea Blvd, Scottsdale, AZ 85259, USA
[4]School of Computing, Informatics, and Decision Systems Engineering, Arizona State University, Tempe, AZ, USA
[5]Barrett, The Honors College, Arizona State University, Tempe, AZ, USA

## Abstract

*Purpose:* To assess mean shear hepatic stiffness calculations using various region of interest (ROI) techniques, a new inversion algorithm, and a confidence threshold mask.
*Methods:* Seventy-three patients (49 with abnormal liver function tests/known chronic liver disease and 24 healthy liver transplant donors) underwent liver biopsy and magnetic resonance elastography (MRE). MRE data processed with the current inversion algorithm [multiscale direct inversion (MSDI)] was assessed using 2 ROI methods (single vs. triple). The data were then reprocessed using the new inversion algorithm (multimodel direct inversion [MMDI]) Hepatic stiffness calculations were performed using a single (70%) ROI method, with/without a 95% confidence threshold mask, and compared with MSDI.
*Results:* For MSDI, average stiffness difference between single and triple ROI methods was not statistically significant by the 2-sample *t* test [0.15 kilopascals (kPa); *P* = .77]. For the 2 algorithms, there was little difference in average stiffness measurements of MSDI and MMDI (mean, 0.32 kPa; 9%) using a confidence mask with good agreement [intraclass correlation coefficient (ICC), 0.986 (95% CI 0.975–0.994)]. Use of the confidence mask showed excellent consistency and less variance [ICC, 0.995 (95% CI 0.993–0.998)] compared to either the inter-observer or intra-observer freehand technique.
*Conclusion:* MRE analysis showed no significant difference between the 2 freehand ROI techniques. With a 9% average kPa variance, stiffness measurements for MSDI and MMDI were also not significantly different. The use of the confidence mask reduces calculated stiffness variability, which impacts the use of MRE for assessing therapy response and initial/longitudinal assessment of chronic liver disease.

**Key words:** Cirrhosis—Liver donor—Liver elastography—Magnetic resonance elastography—Magnetic resonance imaging

## Abbreviations

| | |
|---|---|
| ICC | Intraclass correlation coefficient |
| kPA | Kilopascals |
| MMDI | Multimodel direct inversion |
| MRE | Magnetic resonance elastography |
| MSDI | Multiscale direct inversion |
| ROI | Region of interest |

Hepatic cirrhosis is the second leading gastrointestinal cause of death, with a 50% 5-year mortality [1]. It was once thought to be a progressive, irreversible process; however, increasing evidence indicates that the earlier stages are treatable and reversible with appropriate antifibrotic therapy [2–5]. Thus, there is great need for a noninvasive alternative to liver biopsy, which is the current standard for diagnosis but is painful and has attendant morbidity and mortality [6–9].

Magnetic resonance elastography (MRE) is a novel, noninvasive technique with proven efficacy in the detection and stratification of hepatic fibrosis [10–17]. MRE uses an active/passive pneumatic driver system to
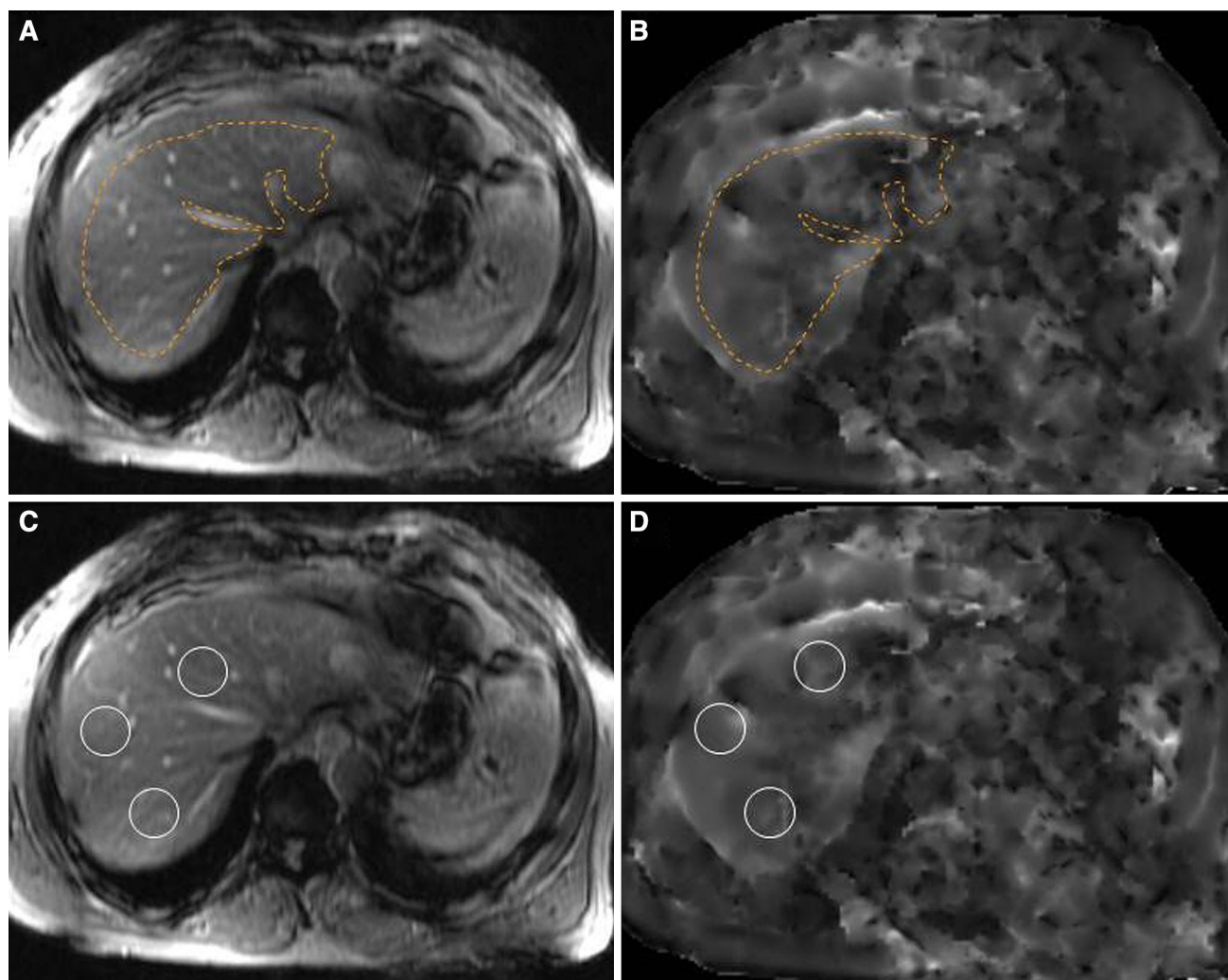
*Correspondence to:* Alvin C. Silva; *email:* silva.alvin@mayo.edu

**Fig. 1.** Comparison of ROI techniques (MSDI). **A** MRE anatomy image with representative single freehand ROI avoiding the liver periphery, large central vessels, and areas of wave interference, including approximately 70% of the central liver. **B** The same ROI drawn on MRE anatomy image (**A**) is copied and pasted onto the elastogram image. **C** MRE anatomy image with representative 3 freehand ROIs, avoiding the liver periphery, large central vessels, and areas of wave interference. **D** The same 3 ROIs drawn on the MRE anatomy image (**C**) are copied and pasted onto the elastogram image (**D**).

produce acoustic shear waves that are first propagated in the liver. A modified phase-contrast sequence is then used to detect the longitudinal wave distribution patterns which are subsequently processed with an inversion algorithm. Multimodel direct inversion (MMDI) is a new algorithm that converts wave image information into a quantified map of tissue stiffness called an *elastogram*. This MRE technique enhancement has several improvements over the prior algorithm (the multiscale direct inversion [MSDI]), including superior resolution, less noise, and shorter processing time.

From the elastogram, stiffness calculations [in kilopascals (kPa)] for MSDI have been generated by various methods [17–19], but these are more commonly performed by 1 of two techniques: (1) a single large region of interest (ROI) drawn around the entire liver; or (2) at least three smaller circular ROIs strategically placed within the liver. However, in conjunction with the advent of the MMDI algorithm, another MRE development is the semiautomated 95% confidence threshold mask, which is designed to help localize regions of reliable information on the elastogram for ROI placement [20].

Prior studies have evaluated the efficacy of MRE in patients with liver fibrosis, but to our knowledge no investigations have directly compared differences in hepatic stiffness measurements between the MMDI and the MSDI inversion algorithms. Thus, it is unclear whether modification with MMDI is necessary for currently suggested cutoff values for discriminating normal from diseased liver or for stratifying the various histologic liver fibrosis stages with MSDI. Furthermore, while current stiffness measurement techniques involve the freehand
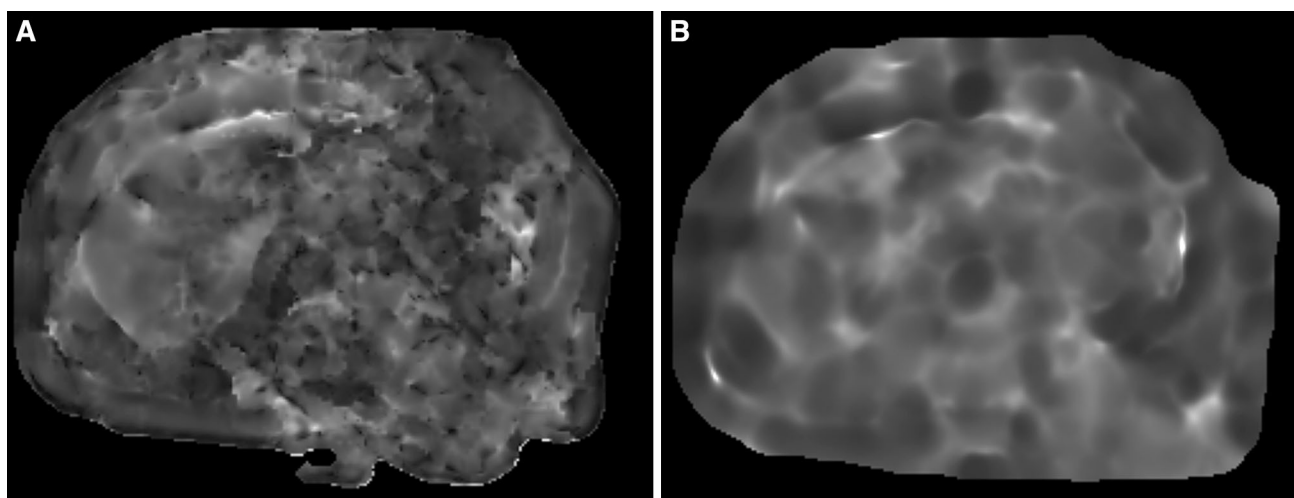
**Fig. 2.** MRE inversion algorithms. **A** Elastogram generated with the current (MSDI) algorithm. **B** Elastogram generated with the new (MMDI) algorithm. Note that there is relatively less noise and fewer artifacts with MMDI. MMDI uses a smaller processing kernel relative to MSDI and generates a smoother result by applying a more appropriate model to the acquired data set.

drawing of either a single large ROI or multiple smaller circular ROIs, no prior studies have compared these freehand techniques with the semiautomated confidence threshold mask. Thus, the purpose of this study was to determine whether any significant differences in stiffness calculations exist between the freehand single and the 3-circle ROI methods, and between MSDI and MMDI algorithms. In addition, inter- and intra-observer variability was assessed between 2 measurement techniques, the freehand ROI (single or multiple) vs. the confidence threshold mask ROI.

## Methods

This study was approved by the Institutional Review Board. The acquisition of informed consent was waived because of the retrospective nature of the study.

### Subjects

A total of 73 consecutive patients with both a liver biopsy and MRE completed within 35 days of each other were identified from our hepatobiliary and transplants clinics between January 1, 2011, and December 31, 2012. The cohort included 49 patients (28 men; 21 women) with abnormal liver function or chronic liver disease as well as 24 healthy liver transplant donors (16 men; 8 women).

### Liver histopathology

All histologic analysis was performed by a single hepatopathologist for whom MRE results and clinical information were masked. Standard classification systems were used for fibrosis staging (METAVIR), nonalcoholic fatty liver disease, and cholestatic liver disease [21].

### MRE technique

A 1.5 T magnetic resonance (GE Signa HDx14.0, Milwaukee, Wisconsin) with 8-channel surface coil was used for all examinations. A combination of active and passive audio driver system produced mechanical shear waves (60 Hz) that were transmitted into the liver, which was then imaged with a modified phase-contrast sequence (wave image) and processed with an inversion algorithm (MSDI or MMDI) to generate a quantitative image of shear stiffness (elastogram) in kPA.

### ROI comparison

For the current algorithm (MSDI), a single experienced observer, for whom histopathology results were masked, calculated MRE measurements on all examinations using the average from 4 hepatic slice locations with the following two methods: (1) 1 freehand ROI that encompassed the central approximately 70% of a liver slice acquisition; and (2) 3 circular ROIs (2.0 cm$^2$) (Fig. 1). In both cases, care was taken to avoid larger vessels and wave reflection/interference. These subjectively assessed values were compared with the relatively objective values as established by the 95% confidence threshold mask. Data analysis was conducted via a linear regression model and the 2-sample $t$ test.

### Inversion algorithm comparison

The MRE data of each patient was processed twice, once with the current inversion algorithm (MSDI) and then once with the new inversion algorithm (MMDI) (Fig. 2). The MMDI algorithm performs multiple polynomial fits to the displacement data and uses a statistical F test to

select the best fit. The algorithm reports the R-squared value from the least squares fit as the confidence mask. Additionally, MMDI uses a total least squares to remove the longitudinal wave so that the remaining shear wave satisfies the Helmholtz equation. Typical processing times for the MSDI and MMDI algorithms on the GE host computer are 40 and 10 s/per slice, respectively. Mean shear hepatic stiffness values in kPa were then calculated using the average from 4 slices in the liver to create the following data sets (Fig. 3):

(a) Observer 1: freehand single ROI using MSDI;
(b) Observer 2: freehand single ROI using MSDI;
(c) Observer 2: freehand single ROI using MSDI; repeated 2 weeks later to avoid memory bias;

(d) Observer 2: confidence threshold mask ROI using MMDI;
(e) Observer 2: confidence threshold mask ROI using MMDI; repeated 2 weeks later to avoid memory bias;
(f) $(f_1 - f_2)$Observer 2: the same confidence threshold mask ROI copied to the same location for both MSDI ($f_1$) and MMDI ($f_2$).

Intraclass correlation coefficients (ICCs) were calculated to assess inter- and intra-observer variability, and Bland–Altman statistical analysis was used to assess agreement. All statistical analyses were performed using SAS 9.1 (SAS Institute Inc, Cary, North Carolina).
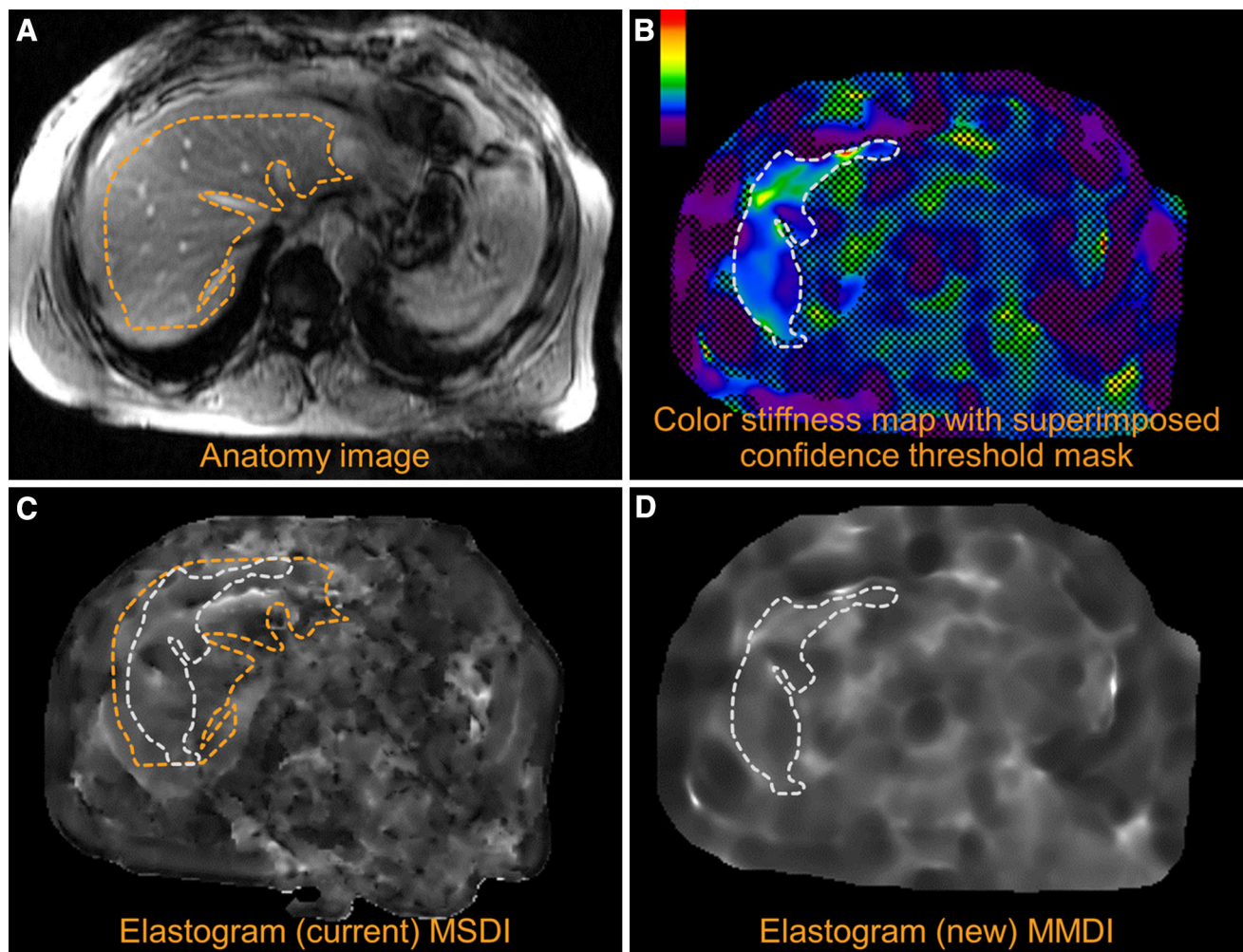


**Fig. 3.** ROI Data Sets. **A** MRE anatomy image with representative single freehand ROI avoiding the liver periphery, large central vessels, and areas of wave interference, including up to approximately 70% of the central liver; used to generate data sets "a" through "c." **B** ROI drawn on color stiffness map with superimposed confidence threshold mask highlighting valid regions with adequate signal-to-noise ratio; used to generate "d" through "f₁" and "f₂" data sets. **C** Elastogram (MSDI) image with freehand ROI (*orange dashed outline*) and confidence threshold mask ROI (*white dashed outline*). **D** Elastogram (MMDI) with confidence threshold mask ROI (**B**) copied and pasted onto image.
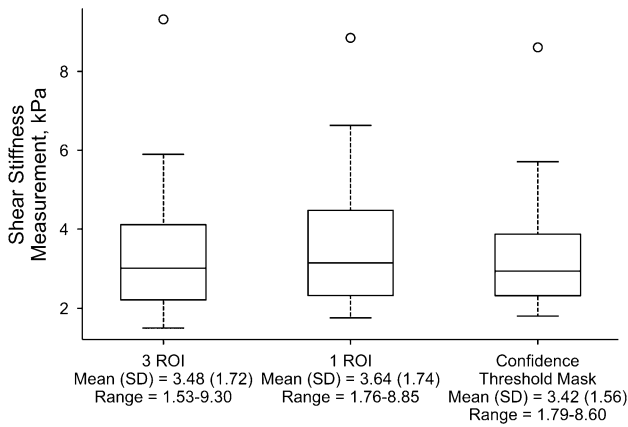
**Fig. 4.** Box plot depicting variance in shear stiffness measurements. Measurements were made using freehand 3-circle ROIs, 1-circle ROI (70%), and confidence threshold mask methods.

**Table 1.** ROI comparison: differences in stiffness measurements

| Pairwise 2-sample $t$ test | a and b[a] | a and c[b] | b and c[c] |
| --- | --- | --- | --- |
| $P$ value | .77 | .90 | .66 |

[a]Comparison of the freehand single region of interest (ROI) method (a) and the 3-circle ROI method
[b]Comparison of the freehand single ROI method and confidence threshold mask
[c]Comparison of the 3-circle ROI method and confidence threshold mask

## Results

### ROI comparison

For MSDI, the mean stiffness measurement using the 3-circle ROI was 3.48 kPa (SD 1.71 kPa) (range 1.53–9.30 kPa); while for the single freehand ROI, it was 3.63 kPa (SD 1.73 kPa) (range 1.76–8.85 kPa) (Fig. 4). When these stiffness measurements were compared to those defined by the 95% confidence threshold mask, there was slightly stronger correlation and higher $R^2$ value with the single than with the 3-circle ROI (Fig. 5); however, pairwise 2-sample $t$ test results showed no significant difference among the 3 techniques (Table 1).

### Inversion algorithm comparison

The mean (SD) and median (kPa) for each data set are shown in Table 2. With Bland–Altman plots (Fig. 6), the mean (SD) of difference in stiffness measurements was greatest between 2 observers (−0.5 and 0.61; data set "a" vs. data set "b"); followed by that of a single observer

(−0.11 and 0.37; data set "b" vs. data set "c"); and least with utilization of the confidence threshold mask (−0.05 and 0.18; data set "d" vs. data set "e"). For MSDI, the ICC showed less intra-observer variability [ICC, 0.978 (95% CI 0.953–0.988)] compared to inter-observer variability [ICC, 0.923 (95% CI 0.885–0.950)] (Fig. 7). In addition, excellent correlation and less variance on repeat MRE was found with the confidence threshold mask [ICC, 0.995 (95% CI 0.993–0.998)] than with the freehand single ROI technique [ICC, 0.978 (95% CI 0.953–0.988)] (Fig. 7). The difference in average shear stiffness between MSDI and MMDI algorithms using the confidence threshold mask method was 0.32 kPA (9%).

## Discussion

MRE cutoff values for detecting and staging hepatic fibrosis [10–17, 22–24] and inflammation [25–27] have largely been performed using the MSDI algorithm. However, as the MRE technique continues to evolve, MMDI has been developed for its relative improved resolution, as well as for its decreased image noise and processing time. The decreased noise was particularly evident on qualitative visual inspection (Fig. 2), which was corroborated by a relatively smaller SD. With respect to average quantitative results, this study showed that the calculated stiffness difference between the 2 algorithms was relatively small (9%), with excellent correlation (ICC, 0995). Published results indicate that same-patient MRE repeatability can range from 22% to 37%
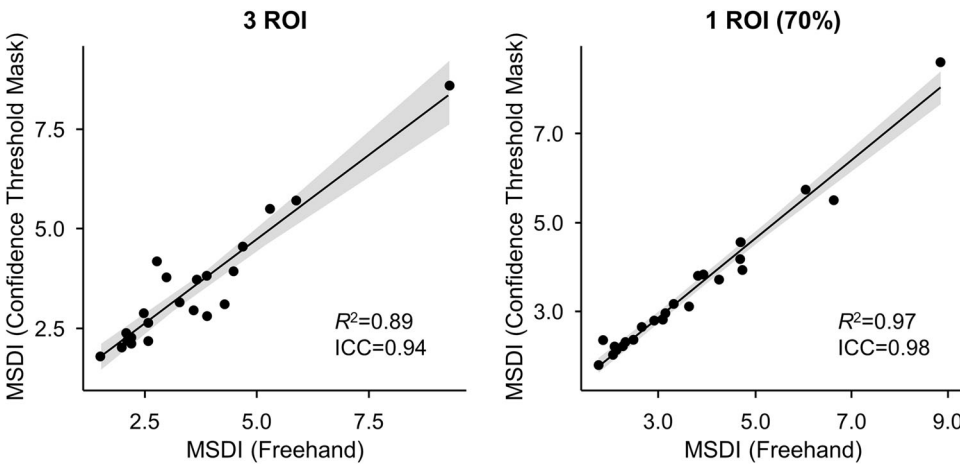


**Fig. 5.** Linear regression model. **A** Calculated stiffness values by freehand 3-circle ROI vs. confidence threshold mask ($R^2$, 0.89; ICC, 0.94). **B** Calculated stiffness values by freehand 1-circle ROI (70%) vs. confidence threshold mask ($R^2$, 0.97; ICC, 0.98).

**Table 2.** Inversion algorithm comparison: shear stiffness values for data sets

| Variable | a: MSDI (Freehand [Obs 1]) | b: MSDI (Freehand [Obs 2]) | c: MSDI (Freehand [Obs 2]) | d: MMDI (Mask[a] [Obs 2]) | e: MMDI (Mask[a] [Obs 2]) | $f_1$: MSDI (Mask[a] [Obs 2]) | $f_2$: MMDI (Mask[a] [Obs 2]) |
|---|---|---|---|---|---|---|---|
| Mean (SD) | 3.24 (1.74) | 3.64 (1.39) | 3.75 (1.32) | 3.63 (1.44) | 3.63 (1.44) | 3.95 (1.55) | 3.63 (1.44) |
| Median | 4.14 | 3.02 | 3.16 | 3.15 | 3.05 | 3.32 | 3.15 |

MMDI, multimodel direct inversion; MSDI, multiscale direct inversion; Obs, observer
[a]Values are in kilopascals (kPa)
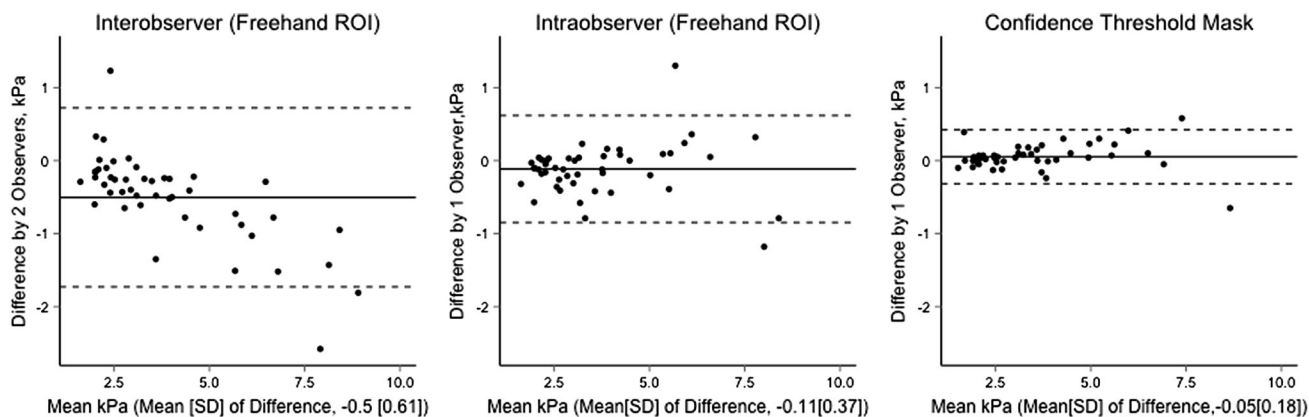[b]Mask indicates confidence threshold mask



**Fig. 6.** Bland-Altman plots of freehand (Inter-observer, Intra-observer) ROI vs. Confidence threshold mask ROI. Mean (SD) of difference in kPa for freehand inter-observer ROI, −0.50 (0.61); for freehand intra-observer ROI, −0.11 (0.37); and for confidence threshold mask ROI, −0.05 (0.18). *Center unbroken line* indicates mean; *top dashed line* indicates mean plus 2SD; and *bottom dashed line* indicates mean minus 2SD.
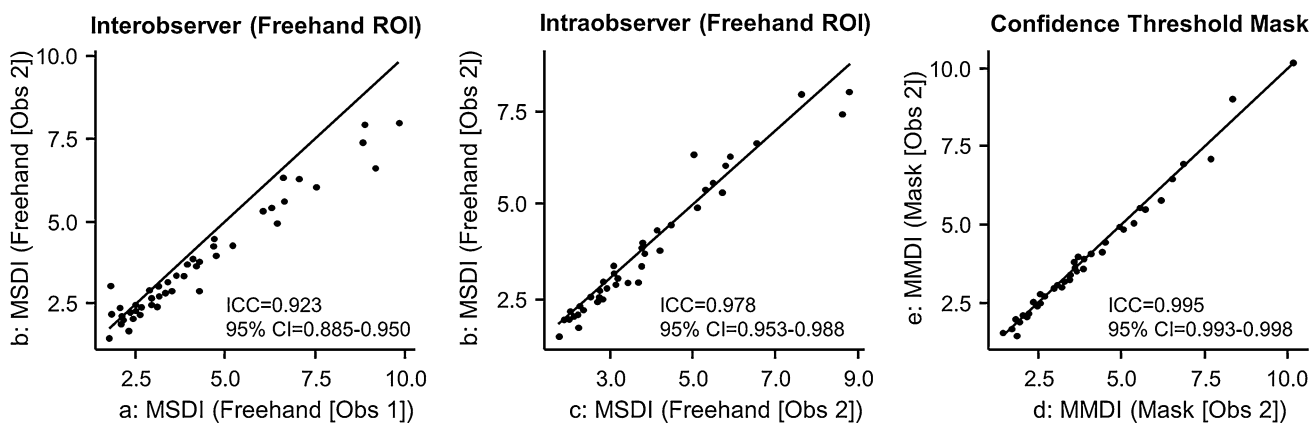


**Fig. 7.** Intraclass correlation coefficient (ICC) of Freehand Inter-observer ROI and freehand intra-observer ROI vs. confidence threshold mask ROI. Freehand inter-observer ROI ICC, 0.923 (95% CI 0.885–0.950); freehand intra-observer ROI ICC, 0.978 (95% CI 0.953–0.988); and confidence threshold mask ROI ICC, 0.995 (95% CI 0.993–0.998).

[23, 28], so the new algorithm should have only minor impact on current cutoff threshold values and variability. However, as both MSDI and MMDI are commercially available, reporting the specific inversion algorithm used in future studies would be beneficial.

Prior to the introduction of the semiautomated 95% confidence threshold mask, the reporting of hepatic tissue stiffness remained a subjective process, requiring meaningful experience for visually determining appropriate ROI placement. Thus, this placement required delineation of the specific methodology in the published literature, as the methodology had an impact on the variability of calculated measurements [18–20, 28]. For example, the reader had to be able to identify regions

that had appropriate signal-to-noise and wave amplitude, without confounding multipath wave interference artifacts, for each and every MRE slice acquisition, all of which was realized by the threshold mask. When repeated measurements were compared, this study showed that utilization of the confidence threshold mask had the least absolute kPa difference and SD (Fig. 6), as well as the highest correlation (Fig. 7) compared to the freehand ROI technique, regardless of performance by the same observer or performance by two different observers. Use of the confidence threshold mask should thus improve inter-patient and serial intra-patient measurement standardization. In addition, consistent utilization of the confidence threshold mask could potentially allow for improved precision when different investigations in the published literature are compared, perhaps mitigating some of the variability introduced by differences in reader training and subjective perception. Although not specifically investigated in this study, the time required to achieve proficiency has been much shorter, in our experience, with the confidence threshold mask than with the subjective, freehand techniques.

If a confidence threshold mask is not available, various methods have been reported with respect to the number, size, and location of ROI placement [17–20, 28], but these are typically performed with a single large ROI rather than several small ROIs. Our results indicate that, although there was higher correlation for the single large ROI technique (Fig. 5), it was not statistically significant (Table 1). This finding differs from those of Lee et al. [19], who reported a significantly higher ICC for the single large ROI than for multiple small ROIs. However, Lee et al. only evaluated normal livers, whereas we included patients with chronic liver disease with greater heterogeneity in hepatic parenchymal changes.

In addition to the retrospective design and small sample size of this study, it had other limitations. All MRE examinations were performed on 1 of 2 scanners from a single vendor. Since this technique is now available on other magnetic resonance platforms, the results may not necessarily translate to a general clinical practice with magnetic resonance scanners from different vendors. In addition, we were unable to directly analyze the effect of different magnet strengths (i.e., 1.5 vs. 3 T) because 3T MRE was unavailable at our institution. However, since hepatic stiffness values in a preliminary study of healthy volunteers at 3 T have been shown to be similar to published 1.5 T values [29], we would expect the new algorithm and confidence threshold mask to have similar results.

In conclusion, previously established hepatic stiffness threshold cutoff values should not be adversely affected by the new inversion algorithm (MMDI), which has excellent correlation and an overall 9% average difference compared with MSDI. The introduction of the objective confidence threshold mask improves measurement consistency over that of the current subjective freehand techniques, thus increasing the reliability of MRE for clinical indications as well as for interinvestigation comparisons.

## References

1. Jepsen P, Vilstrup H, Andersen PK, Lash TL, Sorensen HT (2008) Comorbidity and survival of Danish cirrhosis patients: a nationwide population-based cohort study. Hepatology 48(1):214–220
2. Wan Y, Tang MH, Chen XC, et al. (2014) Inhibitory effect of liposomal quercetin on acute hepatitis and hepatic fibrosis induced by concanavalin A. Braz J Med Biol Res 47(8):655–661
3. Li J, Li X, Xu W, et al. (2014) Antifibrotic effects of luteolin on hepatic stellate cells and liver fibrosis by targeting AKT/mTOR/p70S6K and TGF$\beta$/Smad signalling pathways. Liver Int. doi: 10.1111/liv.12638
4. Jobara K, Kaido T, Hori T, et al. (2014) Whey-hydrolyzed peptide-enriched immunomodulating diet prevents progression of liver cirrhosis in rats. Nutrition 30(10):1195–1207
5. Giannitrapani L, Soresi M, Bondi ML, Montalto G, Cervello M (2014) Nanotechnology applications for the therapy of liver fibrosis. World J Gastroenterol 20(23):7242–7251
6. Rey JW, Jahn-Eimermacher A, Doernberger V, et al. (2014) To biopsy or not to biopsy: evaluation of a large German cohort of patients with abnormal liver tests of unknown etiology. Digestion 89(4):310–318
7. Nalbantoglu I, Brunt EM (2014) Role of liver biopsy in nonalcoholic fatty liver disease. World J Gastroenterol 20(27):9026–9037
8. Perrault J, McGill DB, Ott BJ, Taylor WF (1978) Liver biopsy: complications in 1000 inpatients and outpatients. Gastroenterology 74(1):103–106
9. Thampanitchawong P, Piratvisuth T (1999) Liver biopsy: complications and risk factors. World J Gastroenterol 5(4):301–304
10. Guo Y, Parthasarathy S, Goyal P, et al. (2014) Magnetic resonance elastography and acoustic radiation force impulse for staging hepatic fibrosis: a meta-analysis. Abdom Imaging. doi:10.1007/s00261-014-0137-6
11. Venkatesh SK, Ehman RL (2014) Magnetic resonance elastography of liver. Magn Reson Imaging Clin N Am 22(3):433–446
12. Friedman SL, Rockey DC, Bissell DM (2007) Hepatic fibrosis 2006: report of the Third AASLD Single Topic Conference. Hepatology 45(1):242–249
13. Yeh WC, Li PC, Jeng YM, et al. (2002) Elastic modulus measurements of human liver and correlation with pathology. Ultrasound Med Biol 28(4):467–474
14. Muthupillai R, Lomas DJ, Rossman PJ, et al. (1995) Magnetic resonance elastography by direct visualization of propagating acoustic strain waves. Science 269(5232):1854–1857
15. Rouviere O, Yin M, Dresner MA, et al. (2006) MR elastography of the liver: preliminary results. Radiology 240(2):440–448
16. Huwart L, Peeters F, Sinkus R, et al. (2006) Liver fibrosis: noninvasive assessment with MR elastography. NMR Biomed 19(2):173–179
17. Yin M, Talwalkar JA, Glaser KJ, et al. (2007) Assessment of hepatic fibrosis with magnetic resonance elastography. Clin Gastroenterol Hepatol 5(10):1207–1213
18. Mitsufuji T, Shinagawa Y, Fujimitsu R, et al. (2013) Measurement consistency of MR elastography at 3.0 T: comparison among three different region-of-interest placement methods. Jpn J Radiol 31(5):336–341
19. Lee DH, Lee JM, Han JK, Choi BI (2013) MR elastography of healthy liver parenchyma: normal value and reliability of the liver stiffness value measurement. J Magn Reson Imaging 38(5):1215–1223
20. Dzyubak B, Glaser K, Yin M, et al. (2013) Automated liver stiffness measurements with magnetic resonance elastography. J Magn Reson Imaging 38(2):371–379
21. Goodman ZD (2007) Grading and staging systems for inflammation and fibrosis in chronic liver diseases. J Hepatol 47(4):598–607

22. Venkatesh SK, Wang G, Lim SG, Wee A (2014) Magnetic resonance elastography for the detection and staging of liver fibrosis in chronic hepatitis B. Eur Radiol 24(1):70–78
23. Bohte AE, Garteiser P, De Niet A, et al. (2013) MR elastography of the liver: defining thresholds for detecting viscoelastic changes. Radiology 269(3):768–776
24. Runge JH, Bohte AE, Verheij J, et al. (2014) Comparison of interobserver agreement of magnetic resonance elastography with histopathological staging of liver fibrosis. Abdom Imaging 39(2): 283–290
25. Kim D, Kim WR, Talwalkar JA, Kim HJ, Ehman RL (2013) Advanced fibrosis in nonalcoholic fatty liver disease: noninvasive assessment with MR elastography. Radiology 268(2):411–419
26. Chen J, Talwalkar JA, Yin M, et al. (2011) Early detection of nonalcoholic steatohepatitis in patients with nonalcoholic fatty liver disease by using MR elastography. Radiology 259(3):749–756
27. Salameh N, Larrat B, Abarca-Quinones J, et al. (2009) Early detection of steatohepatitis in fatty rat liver by using MR elastography. Radiology 253(1):90–97
28. Hines CD, Bley TA, Lindstrom MJ, Reeder SB (2010) Repeatability of magnetic resonance elastography for quantification of hepatic stiffness. J Magn Reson Imaging 31(3):725–731
29. Mannelli L, Godfrey E, Graves MJ, et al. (2012) Magnetic resonance elastography: feasibility of liver stiffness measurements in healthy volunteers at 3T. Clin Radiol 67(3):258–262